PROCEEDINGS OF SCIENCE

Nuclei identification performances studies of the Plastic Scintillator Detector (PSD) for the future HERD space mission.

D. Serini,[a,*] **F. Alemanno**[*,c,d] **C. Altomare,**[a] **P. Bernardini,**[e,f] **F.C.T. Barbato,**[c,d] **I. Cagnoli,**[c,d] **E.Casilli,**[e,f] **P. W. Cattaneo,**[g] **A. Comerma,**[h,i] **I. De Mitri,**[c,d] **F. De Palma,**[e,f] **C. De Vecchi,**[g] **A. Di Giovanni,**[c,d] **M. Di Santo,**[c,d] **M.Donetti,**[j] **A. Espinya,**[h,i] **L. Di Venere,**[a] **M. Fernandez Alonso,**[c,d] **G. Fontanella,**[c,d] **P. Fusco,**[a,b] **F. Gargano,**[a] **D. Gascon,**[h] **S.Gomez,**[h,i] **E. Ghose,**[e,f,k] **D. Guberman,**[h,i] **D. Kyratzis**[†,c,d] **F. Licciulli,**[a] **F. Loparco,**[a,b] **S. Loporchio,**[a,b] **L. Lorusso,**[a,b] **J. Mauricio,**[h] **M.N. Mazziotta,**[a] **A.Mereghetti,**[j] **S. Nicotri,**[a] **G. Panzarini,**[a,b] **A. Parenti,**[c,d] **R. Pillera,**[a,b] **M. Pullia,**[j] **A. Rappoldi,**[g] **G. Raselli,**[g] **M. Rossella,**[g] **A. Sammukh,**[h] **A. Sanuy,**[h] **S. Savazzi,**[j] **L. Silveri,**[c,d] **A. Smirnov,**[c,d] **A. Surdo,**[e,f] **R. Triggiani**[a] **and L. Wu**[‡,c,d] **for the HERD collaboration**

[a] *Istituto Nazionale di Fisica Nucleare, Sezione di Bari, via Orabona 4, I-70126 Bari*

[b] *Dipartimento di Fisica "M. Merlin", dell'Università e del Politecnico di Bari, via Amendola 173, I-70126 Bari, Italy*

[c] *Gran Sasso Science Institute (GSSI), viale Francesco Crispi 7 I-67100 L'Aquila, Italy*

[d] *Istituto Nazionale di Fisica Nucleare (INFN)—Laboratori Nazionali del Gran Sasso, via Giovanni Acitelli 22, I-67100, L'Aquila, Italy*

[e] *Istituto Nazionale di Fisica Nucleare (INFN)—Sezione di Lecce, via Arnesano 0, I-73100, Lecce, Italy*

[f] *Dipartimento di Matematica e Fisica "Ennio de Giorgi", Università del Salento, via Arnesano 0, I-73100, Lecce, Italy*

[g] *Istituto Nazionale di Fisica Nucleare (INFN)—Sezione di Pavia, via Agostino Bassi 6, I-27100, Pavia, Italy*

[h] *Institute of Cosmos Sciences - University of Barcelona (ICC-UB), Carrer de Martí i Franquès, 1, 08028 Barcelona, Spain*

[i] *Serra Húnter Fellow, Polytechnic University of Catalonia (UPC), Carrer de Jordi Girona, 31, 08034 Barcelona, Spain*

[j] *CNAO Foundation, via Erminio Borloni 1, 27100 Pavia, Italy*

[k] *Università degli studi di Trento, Dipartimento di Fisica, Via Sommarive, 14, 38123 Povo, Trento TN*

E-mail: davide.serini@ba.infn.it

*Now at: Dipartimento di Matematica e Fisica "Ennio de Giorgi", Università del Salento, Lecce, Italy

†Now at: Department of Nuclear and Particle Physics, University of Geneva, CH-1211 Geneva, Switzerland

‡Now at: Institute of Deep Space Sciences, Deep Space Exploration Laboratory, Hefei 230026, China

*Speaker

PoS(ICRC2023)112

The High Energy cosmic-Radiation Detection (HERD) facility onboard the Chinese Space Station will provide high quality data on charged cosmic rays from few GeV to PeV energies and gamma rays above 100 MeV. HERD will employ a Plastic Scintillator Detector (PSD) to discriminate charged from neutral particles to help identify gamma rays and to measure the nuclei charge up to iron. For these reasons, the HERD PSD needs to have high detection efficiency ($\sim$ 99.998%) and a good charge resolution ($\sim$ 30% at low Z). During 2022 and 2023, beam test campaigns were performed at CERN and at CNAO (Centro Nazionale di Adroterapia Oncologica) in Italy, aimed at studying the overall performance of the PSD detector. A prototype detector composed of 8 plastic scintillator trapezoidal bars of two different lengths was equipped with Silicon Photomultipliers (SiPMs) arranged in different positions along the bars. We tested SiPM of different sizes to increase the dynamic range and study the charge resolution in the range of Z between 1 and $\sim$ 26. The prototype was irradiated with relativistic protons and pions at CERN PS, an ion beam at CERN SPS and with low momentum protons and C ions (with energy release similar to those of high-Z relativistic particles) at CNAO. In this work we present and compare the results from these campaigns. Moreover, we present a characterization of plastic scintillator detectors for the future generation of space missions, with respect to their capabilities for nuclei identification, in terms of quenching effects.

38th International Cosmic Ray Conference (ICRC2023)
26 July - 3 August, 2023
Nagoya, Japan

1. Introduction

The High Energy Cosmic Radiation Detection facility (HERD) is a cosmic-ray experiment that will be installed onboard the future Chinese Space Station (CSS), aimed at providing high-quality data on charged cosmic rays in an energy range spanning from a few GeV to PeV, as well as gamma rays with energies above 100 MeV [1]. The outermost instrument subsystem onboard on HERD will be the Plastic Scintillator Detector (PSD) that will surround the entire facility. Plastic scintillator detectors are commonly employed in satellite experiments as an anti-coincidence system for gamma rays and for identifying charged nuclei [2, 3]. The PSD is assigned several important tasks to accomplish. Firstly, it will contribute to the L0 trigger logic by providing the veto signal necessary for selecting gamma rays with energies below 10 GeV. Additionally, it will provides an independent charge measurement of cosmic ray nuclei, as the energy released (and thus scintillation light yield) is proportional to the square of the incoming particle's atomic number (Z^2). To fulfill these tasks successfully, the PSD must meet stringent requirements in terms of an high efficiency in detecting charged particles ($> 99.8\%$), a wide dynamic range to identifying nuclei up to at least iron and a charge resolution below 30% [4, 5]. To achieve high performance in terms of detection efficiency and charge resolution, a key requirement for the PSD is a highly segmented geometry to minimize self-veto caused by backscattered charged particles [6]. The proposed configuration for the HERD PSD is based on trapezoidal scintillator tiles coupled to Silicon Photomultipliers (SiPMs). The trapezoidal shape of the tiles is chosen for optimal packaging of the entire detector while SiPMs will be utilized for reading out the scintillation light, replacing the traditional Photomultiplier Tubes (PMTs) commonly used in space missions offering the advantages of more compact detectors with lower power consumption, without sacrificing performance. In 2022 and 2023, beam test campaigns were conducted at CERN and the Centro Nazionale di Adroterapia Oncologica (CNAO) in Pavia to study the overall performance of the PSD. These campaigns aimed to optimize the scintillator geometry and SiPM-based readout, as well as evaluate the prototype's overall performance.

2. Prototypes tested

Beam test campaigns were conducted at CERN in 2022 [7] to evaluate the performance of the PSD and optimize its scintillator geometry and SiPM-based readout. The initial prototype of the PSD underwent testing during the SPS H8 beam test at CERN. The prototype used in the SPS beam test consisted of eight trapezoidal tiles made of `BC404` plastic scintillator. Two variants of these tiles, referred to as "long" (L) and "short" (S), were utilized, measuring 40 cm and 30 cm in length, respectively. Each trapezoidal tile was equipped with Hamamatsu SiPMs, namely the $1.3 \times 1.3\,\mathrm{mm}^2$ (model `S14160-1315`) and $3 \times 3\,\mathrm{mm}^2$ (model `S14160-3015`) SiPMs, referred to as S1 (small SiPMs) and S3 (large SiPMs), respectively. Two Printed Circuit Boards (PCBs) equipped with three SiPMs connected in parallel are placed on the larger face. These PCBs housed SiPMs of both sizes (S1 and S3). In addition, two SiPMs connected in parallel are placed on the two smaller sides of the bar ("end-cap", hereafter E). During the SPS beam test, additional HERD sub-detectors were also tested along the beam line. A picture of the prototype tested at CERN SPS H8 is shown in Fig. 1.

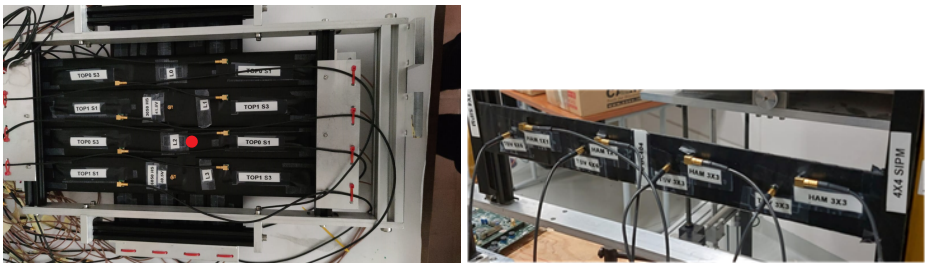

Figure 1: *On the left*: picture of the PSD prototype compose of 4 long (L) and 4 short (S) trapezoildal tiles tested at CERN SPS H8. The prototype was irradiated in the position indicated by the red point, between the L2 and the S1 bar. *On the right*: picture of the tested trapezoidal tile at CNAO.

Further beam tests were conducted at the Centro Nazionale Adroterapia Oncologica (CNAO) in 2023 using a smaller PSD prototype consisting of a single scintillator trapezoidal tile[1]. The prototype tested at CNAO has been equipped with different SiPMs with different area (6.0×6.0, 3.0×3.0 and $1.3 \times 1.3\,\mathrm{mm}^2$) and cell sizes ($50\,\mu$m and $15\,\mu$m). This configuration allowed the large SiPMs to offer higher resolution but a lower dynamic range for detecting low-Z particles, while the small SiPMs provided lower resolution but a higher dynamic range for identifying high-Z particles. The sensors are positioned along the larger face of the tile as shown in the picture in Fig. 1. To ensure uniform light collection, the sensor positioning was optimized using dedicated Monte Carlo simulations [8, 9]. In both beam test campaigns, the PSD prototypes utilized the *HERD-BETA* chip (fiBre trackEr readouT Asic, BETA) as the read-out electronics. The BETA ASIC, developed by the Electronics Instrumentation Service of the Institute of Cosmos Science of the University of Barcelona (ICCUB-SiUB) [10, 11].

3. Beam test at CERN SPS-H8

At CERN SPS-H8, the first PSD prototype was irradiated with a 330 GeV/Z ion beam derived from a 150 GeV/A primary lead beam, impinging onto a Beryllium target with a size of 4 cm, with an ion selection of A/Z = 2.2. The irradiation region spanned the long tile L2 and the short bar S1 of the PSD.-+A trigger system was used to select primary particles with $Z \geq 3$ while the two squared tiles T1 and T2 of $10 \times 10 \times 0.5\,\mathrm{cm}^3$, were placed on the beam axis upstream the beam and downstream of the PSD prototype to monitoring of beam composition and particle fragmentation caused by subsystems between the beam pipe and the PSD prototype. While the ADC channel spectrum of the upstream tile exhibits excellent charge resolution, the PSD prototype spectra did not show the same high charge resolution (maily due to the beam fragmentation). To identify signals from primary particles with $Z > 6$, events (in ADC channels) from the T1 tile were correlated with those from the PSD L2 bar. In the scatter plot shows in Fig.2, the diagonal spots correspond to the signals from primary particles, while the tails represent energy released by daughter particles. By performing a multi-gaussian fit on the T1 spectrum, events associated with each primary beam particle were selected. The projection slice of the scatter plot for each primary ion provided the signal observed by the PSD L2 tile for that specific primary ion. In the right plots

[1]The CNAO is an italian canter for hadrontherapy and it has an experimental area with p and C beam accelerated up to few hundred MeV that can be used to mimic high Z particle due to higher energy loss.

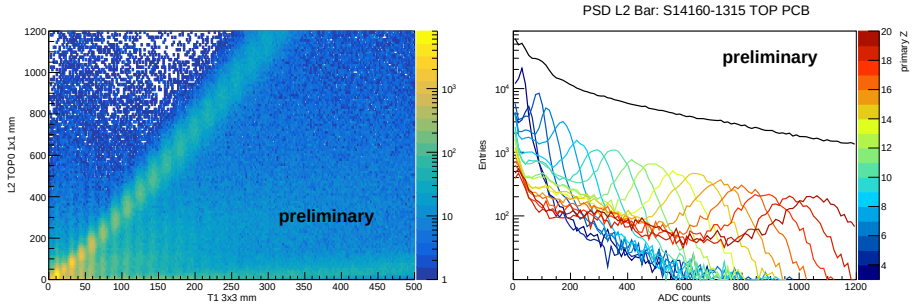

Figure 2: *On the left*: Scatter plot with the correlated data (ADC counts) of the squared tile T1 and the trapezoidal tile L2 of the PSD prototype (TOP SiPMs - 3×3 PCB). *On the right*: PSD L2 bar overall spectrum over imposed with the spectra generated by each primary particle. These spectra are inferred by the selection performed from the scatter plots. Each color represent a different primary ion Z.

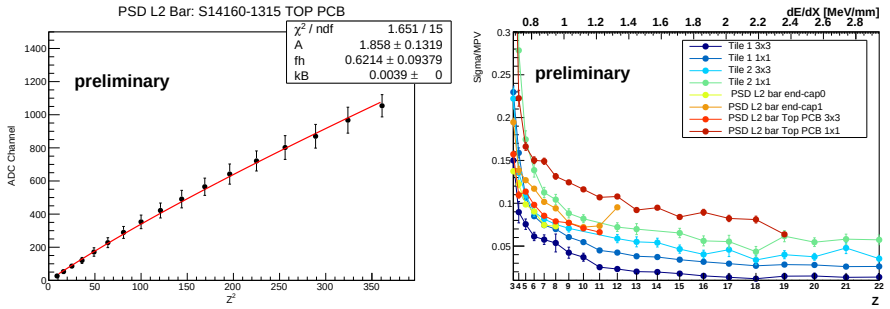

Figure 3: *On the left*: Mean ADC channels as a function of the Z^2 of the different primary ions from the selected signals of the PSD L2 bar correlated with the T1 tile. The red line represents the best-fit curves obtained using "halo-core" formula (Eq. 1) [14]. *On the right*: Resolution evaluated as $R = \frac{\sigma}{MPV}$ for all the detector tested as a function of Z^2 of the different primary ions and their mean energy released (estimated using a Monte Carlo simulation [8, 9]).

of Fig. 2, these spectra are over imposed to the overall count spectra, with each color representing a different primary ion selection. The peak in each spectrum corresponds to primary particles reaching the analyzed scintillator without fragmentation, while the long tails at lower ADC count values represent the energy released by all the daughters generated along the beam line. This data selection procedure enabled the identification of the expected peak ADC channel value for the PSD prototype trapezoidal tiles [7].

The obtained spectra were then used to measure the charge resolution and explore the Birks' saturation effect, which is crucial for accurately calibrating the PSD response [12]. At higher energy losses, a saturation effect is commonly observed in plastic scintillator materials. This saturation effect is described by Birks' law [13], which considers the quenching effects and relates the scintillation light yield dL/dx to the energy deposited dE/dx [14]:

$$\frac{dL}{dx} = A \cdot \frac{(1 - f_h) \cdot \frac{dE}{dx}}{1 + k_b \cdot \frac{dE}{dx}} + A \cdot f_h \frac{dE}{dx} \tag{1}$$

where $dE/dx \propto Z^2$, f_h represents the fraction of energy deposited in the halo, k_b is the Birks constant that depends on the material and governs the strength of the saturation and A is an overall

gain normalization. The plot on the left in Fig. 3 shows the ADC counts as a function of Z^2 for the primary particles observed by the PSD L2 bar. Each point corresponds to a different ion (Li^{3+}, Be^{4+}, B^{5+}, etc.), and the red line represents the best-fit curve obtained using Eq.(1), which shows a very good agreement with the measured data. To assess the PSD prototype's capability to identify nuclei, an estimate of the energy resolution was obtained by fitting the peaks corresponding to different primary Z particles with Gaussian functions. The energy resolution R was calculated as $R = \sigma/MPV$, where σ and MPV are the sigma and mean values of each fitted Gaussian, respectively. Fig. 3 shows the R value as a function of the primary particle's Z for all the different detector prototypes tested (T1 tile, T2 tile, and PSD L2 bar). The second axis on the top shows the expected energy released by each ion, evaluated using Monte Carlo simulations [8, 9]. High-Z particles are better resolved. Furthermore the results show that the smaller SiPMs (e.g.`S14160-1315` - $1.3 \times 1.3 mm^2$) collect less scintillation light, resulting in reduced energy resolution compared to larger SiPMs (e.g., `S14160-3015` - $3 \times 3 mm^2$). However, using smaller sensors allows for an increased dynamic range of the detector to avoid saturating the readout chain for high-Z particles.

4. Beam tests at CNAO

During the CNAO beam test, a single prototype trapezoidal tile of the PSD was irradiated with proton and carbon ion beams accelerated to a few hundred MeV that mimic high Z particles with the higher energy loss. One of the initial tests involved irradiating the tile at different positions to study the uniformity of light collection. The schematic of the prototype, shown on the top of Fig. 4, indicates the two reference SiPMs used for this study. Both SiPMs were Hamamatsu `S14160-3050HS` models with an area of 3.0×3.0 and a cell size of $50\,\mu$m. One SiPM was positioned centrally (circled in red), while the other was placed externally (circled in green) along the larger face of the tile.

The tile was irradiated at 18 different positions along the larger face, with a step size of 2 cm, using a beam of protons at 226.91 MeV. The left plots in Fig. 4 shows the signals collected by the reference SiPMs for all the scanned positions (central and external SiPMs shown on the top and bottom, respectively). Each color represents a different scan position. The right plots show the maximum values evaluated by fitting the spectra with a gaussian as a function of the beam position along the tile. The red lines indicate the distance in terms of σ from the pedestal, revealing that nearly all the collected signals are resolved. Both plots demonstrate significant non-uniformity in light collection, primarily attributed to scintillation light reaching the SiPM without undergoing internal reflection within the trapezoidal tile ("prompt light effect" [8]). Additionally, when the beam directly hit the SiPM, an additional signal was observed due to ionization in the silicon, often resulting in the saturation of the readout chain. These effects can be addressed during flight data acquisition by utilizing a tracking system that provides information about the particle trajectory. This enables the evaluation and compensation of the non-uniformity in light collection.

A second test was performed, irradiating the tile with protons at 228.57 MeV and carbon ions at 259.75 MeV/u in the central position to study the charge resolution for different SiPMs at different gains of the SiPM preamplifier. For each gain the ADC spectra were fitted using a Gaussian function, and the resolution was determined by evaluating following the same methodology discussed in

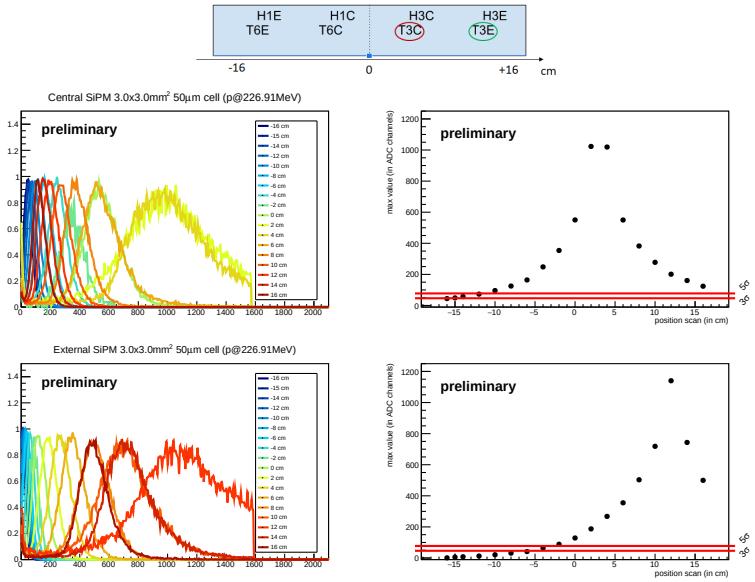

Figure 4: Scan results for studying light collection uniformity. The positioning of two reference SiPMs (S14160-3050HS), along the tile face is shown on the top. The tile was irradiated at 18 different positions, with a step size of 2 cm, using a beam of protons at 226.91 MeV. *Left plots*: signals collected by the reference SiPMs (normalized to the maximum) for all scanned positions, with central and external SiPMs shown at the top and bottom, respectively. Each color represents a different scan position. *Right plots*: maximum values of the signal as a function of the scan position.

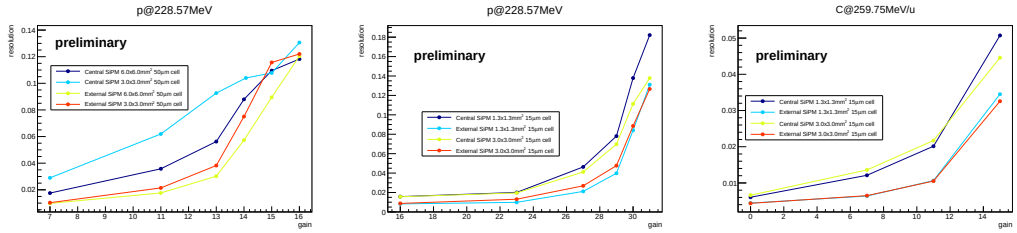

Figure 5: Resolution evaluated by fitting the signals at different gains using a Gaussian function, for the Low-Z SiPMs (50 μm cell sizes) with p at 228.57 MeV (left panel) and for the High-Z SiPMs (15 μm cell sizes) with both p at 228.57 MeV and C at 259.75 MeV/u (central and right panels) impinging the trapezoidal tile in the central position.

section 3. The results for all the SiPMs are presented in the plots of Fig. 5. In particular, the left plot shows the results obtained for SiPMs with 50μm cell sizes when the tile was irradiated in the central position with a proton beam of 228.57 MeV. The tile was equipped with two S14160-3050HS SiPMs with an area of 3.0×3.0 and two S14160-6050HS SiPMs with an area of 6.0×6.0. These SiPMs, with larger cell sizes, generally exhibited higher intrinsic gain, leading to enhanced detection efficiency for Minimum Ionizing Particles (MIPs). However, they were less suitable for detecting high Z particles due to potential saturation of the readout chain. As a result, they can be primarily utilized as "Low-Z SiPMs". On the other hand, the central and right plots in Fig. 5 present the results obtained for SiPMs with 15μm cell sizes when the tile was irradiated in the central position with both the proton and carbon beams. In this case we have considered the signals collected by

the S14160-1315PE SiPMs with an area of $1.3 \times 1.3\,\mathrm{mm}^2$ and the S14160-3015PE SiPMs with an area of 3.0×3.0. These SiPMs, with smaller cell sizes, generally exhibited lower intrinsic gain, optimized for efficient detection of MIPs. However, the lower gain proved advantageous for expanding the dynamic range and enabling detection of heavy ions such as iron. Hence, they can be primarily utilized as "HighZ SiPMs". It is worth noting that all the plots in Fig. 5 consistently exhibit resolution values below 20% for all configurations.

5. Conclusion

The Plastic Scintillator Detector (PSD) plays a crucial role in satellite experiments, serving for γ-identification (charged particle veto) and nuclei identification (charge measurement). In this study, we have presented the main findings from the beam test campaigns conducted at CERN SPS H8 and CNAO, aiming to evaluate the performance of the PSD prototype for particle identification. The various prototypes developed and tested have provided invaluable insights for enhancing the design. The results obtained can be used to define the final geometry of the PSD of the HERD facility and the best configuration for the SiPM positioning in order to satisfy the requirements to be used as charge detector. The preliminary results here presented demonstrate the capability of the prototypes in fulfilling all the necessary requirements for the flight version of the HERD facility.

Acknowledgment

The data acquired at CNAO were obtained thanks to the CNAO experimental facility, which was built in collaboration with INFN.

The authors would like to thank all the technical staff of the INFN Bari and in particular M. Mongelli, N. Aprile Ximenes, M. Papagni, F. Maiorano, N. Lacalamita, M. Franco and S. Martiradonna for their fundamental help in the realization of the prototypes.

References

[1] Dong, Y., et al., *PoS*, (2020), **ICRC2019**, 62

[2] Moiseev, A. A., et. al., *Astrop. Phys.*, (2007), **27**, 339.

[3] Yu, Y., et al., *Astrop. Phys.*, (2017), **94**, 1.

[4] F., Gargano, et. al., *Nucl.Instrum. Meth.A*, **164476**, (2020), 983.

[5] Serini, D. *Il nuovo cimento*, (2020), **C 43.2-3**, 1-2

[6] HU, Peng, et al., *Radiation Detection Technology and Methods*, **5** (2021), p. 332–338.

[7] D.Serini, C.Altomare et. al., *IEEExplore special issue*, **IWASI 2023**, (2023), p. 184-189.

[8] Altomare C., Serini D., et al, *Nucl.Instrum.Meth.A*, (2020), **982**, 164479.

[9] Altomare, C., Serini D., et al. *Journal of Physics: Conference Series.*, (2022), 012050.

[10] Perrina, C., et al., *PoS*, (2020), **ICRC2019**, 122.

[11] A. Sanmukh *et al. IEEE*, (2021), **NSS/MIC**, 1-3.

[12] H. Bethe, J. Ashkin, *Experimental Nuclear Physics*, (1953), **64**, 253.

[13] Birks J.B *Proc.Phys.Soc.A*, (1951), **64**, 874-877.

[14] Dwyer, R. and Zhou, D., *Nucl. Instrum. Meth.A*, (1985), **242**, 171-176.